Investigating the effects of vascular patterning on cardiac patch anastomosis

DaLoria Boone

Sarah Goldfarb

George Nageeb

BIOGRAPHICAL SKETCH

NAME: DaLoria Boone

POSITION/TITLE: Student

EDUCATION/TRAINING:

INSTITUTION AND LOCATION	DEGREE	Completion Date MM/YYYY	FIELD OF STUDY
Harvard College, Cambridge, MA	S.B.	Anticipated 05/2022	Bioengineering

Positions and Honors

Engineering Design Problem Solving/Design Cambridge, MA
Student / Professor David Mooney September - December 2020

- Worked with colleagues to learn the engineering design process through teamwork, problem identification, computational modeling, and prototyping
- Engineered a solution for the prevention and mitigation of SARS-CoV-2 transmission for the Harvard Face Mask Committee
- Managed a subgroup focused on testing the fit and comfort of the mask to determine overall mask efficacy
- Summarized our solution and findings into 3 papers in order to be published

BIOGRAPHICAL SKETCH

NAME: Sarah Goldfarb

POSITION/TITLE: Student

EDUCATION/TRAINING:

INSTITUTION AND LOCATION	DEGREE	Completion Date MM/YYYY	FIELD OF STUDY
Harvard College, Cambridge, MA	S.B.	Anticipated 05/2022	Bioengineering

Positions and Honors

Wein Lab, Massachusetts General Hospital Boston, MA
Research Student / Dr. Marc Wein June 2019 - May 2020, Sept. 2020 - present

- Study the effects of parathyroid hormone and small molecule salt-inducible kinase inhibitors on signaling pathways in osteocytes, osteoblasts, osteoclasts, and hepatocytes in mice
- Perform cell culture and treatment, protein collection, mouse dissections, RNA sequencing, qPCR, Western Blotting, and mouse bone marrow extractions
- Recipient of Harvard College Research Program Funding (Summer 2019)
- Awarded Herchel Smith Harvard Research Fellowship (Summer 2021)

ArthurHealth Toronto, ON
Summer Intern / Dr. Raja Rampersaud June - Aug. 2020

- Co-developed a care plan for the general patient experiencing musculoskeletal pain
- Coded and updated the website to make it more functional and easier to navigate
- Communicated physician recommendations—such as post-surgery exercise plans, over-the-counter medication suggestions, and signs and symptoms—to patients

BIOGRAPHICAL SKETCH

NAME: George Nageeb

POSITION/TITLE: Student

EDUCATION/TRAINING:

INSTITUTION AND LOCATION	DEGREE	Completion Date MM/YYYY	FIELD OF STUDY
Harvard College, Cambridge, MA	A.B.	Anticipated 05/2022	Biomedical Engineering

Positions and Honors

Church Lab, Wyss Institute Longwood, MA
Research Student / Dr. George Church *January 2020 - March 2020*

- Worked with PhD students on a project for recapitulating oogenesis *in vitro* using Crispr Cas-9 technologies. Research interrupted by COVID-19

Specific Aims

Motivation: Cardiovascular disease (CVD) is the leading cause of death in both the United States and worldwide [1]. Furthermore, there are approximately 1.5 million myocardial infarctions (MI) in the United States each year and myocardium is one of the least regenerative tissues in mammals [2, 3]. Thus, identifying effective methods to treat and regenerate myocardium is increasingly relevant in the field of tissue engineering.

Thus far, there have been various engineered tissues that have emerged as promising approaches to repair damaged organs. In order to address MI, many researchers have investigated cardiac patches, which are an engineered layer of healthy tissue that is implanted onto the infarct to promote regeneration. Despite the clinical need, the therapeutic application of engineered cardiac tissues has not been achieved, and this is largely due to the lack of functional vascularization in the patches, inability for the tissue to be perfused, and lack of effective integration with host vessels *in vivo* [4, 5].

In order to address this lack of vascularization, researchers have started to engineer vascular networks before implantation through a process called prevascularization. These efforts mostly rely on self-assembly of endothelial cells (ECs) to form connected tubes within cardiac constructs [5, 6, 7, 8]. While these efforts have successfully achieved perfusion *in vivo*, the perfusion was not efficient and the grafts were only partially integrated [5, 6, 7, 8].

Following these experiments, researchers have started to investigate prepatterning the prevascularization designs in order to achieve greater integration. In 2020, Redd et al. showed that a grid pattern of vasculature allowed for better anastomosis and perfusion in infarcted rat hearts, as compared to random vasculature [9]. They also found that this increased anastomosis and perfusion in rat hearts may be attributed to changes in gene expression [9].

To solve the problem of limited anastomosis of cardiac patches, we will develop an *in vivo* murine model to study the effects of the prevascularization pattern on cardiac patch anastomosis.

Hypothesis: Prevascularizing cardiac patches in a striated pattern will cause an upregulation of gene expression associated with vascular development and induce better cardiomyocyte alignment *in vitro*, resulting in earlier anastomosis with host vasculature and better cardiac patch engraftment *in vivo*.

Aim 1: Prepatterning hiPSC-ECs using Laser Induced Forward Transfer (LIFT) to create cardiac patches with various vascular patterns in vitro and testing if printed patches match the expected outcomes.

Aim 2: Testing patterned cardiac patches in vitro for perfusability, thrombogenicity, contractility, and differences in gene expression to ensure their usability for in vivo implantation as tissue matures.

Aim 3: Performing an *in vivo* study in a rat model of myocardial infarction to investigate and compare the efficacy of various cardiac patch patterns.

Impact: Identifying differences in speed and extent of anastomosis between patch patterns may provide insight regarding the effects of endothelial patterning on cardiac patches, thereby addressing an unanswered research question in the field of MI treatment. Furthermore, identifying ideal vasculature patterns for cardiac patches may inform future designs for cardiac patches in humans and have meaningful translational applications.

Research Strategy

Significance: Over 1.5 million Americans suffer from myocardial infarction annually, causing cardiomyocyte death and cardiac fibrosis, thereby impairing heart function [2]. Because the heart is one of the least regenerative organs in humans, with a cardiomyocyte turnover rate of 0.3–1% annually, tissue engineering of cardiac patches has emerged as a promising treatment approach [10].

Due to the high metabolic demands of contracting tissue, cardiac patches require adequate vascularization to provide oxygen and nutrients to the surrounding cells. For this reason, attempts have been made in recent years, to prevascularize cardiac patches such that they can become perfusible shortly after implantation. Such attempts have largely relied on self assembly of vasculature to date. Because cardiac muscle function depends heavily on its unique structural organization, however, it is important to recapitulate both ventricular and vascular geometry for engineering functional cardiac tissue [11].

In 2013, a review of cardiac tissue engineering outlined recent studies of tissue-engineered cardiac patches using various models, scaffold designs, and cell types. At the time, researchers struggled to develop effective cardiac patches due to the challenges associated with providing sufficient oxygen and nutrients to cells. Thus, one of the main challenges in engineering viable cardiac patches has been inducing proper prevascularization to support the nutritional needs of graft cells upon implantation, as well as inducing anastomosis between engineered and native vasculature. Vollert et al. (2013) first demonstrated an approach for inducing tubular channels, suitable for perfusion, in engineered heart tissues (EHT) by imbedding dissolvable alginate fibers within the cell-fibrin-thrombin mixture. With improved technology in gel patterning, however, there is greater potential for prevascularization in EHTs [12].

In 2019, Redd et al. demonstrated that seeding human embryonic stem cell-derived endothelial cells into patterned microchannel networks of collagen matrix, led to sprouting along lumen walls as well as anastomosis with de novo endothelial tubes placed in the matrix. Several studies confirm that prior patterning improves overall graft integration, likely due to topographical signaling which can guide invading vessels. Despite normal ranges of velocity flow in graft vessels, they still do not resemble native coronary structure or organization and they undergo significant geometric restructuring upon implantation. Juhas et al. (2014) have shown that biomimetic structure of aligned muscle fiber architecture may provide structural cues to invading host vasculature and has enhanced engineered skeletal muscle contractility. Future research could utilize a similar biomimetic strategy in emulating cardiomyocyte vascularization for prevascularization of cardiac patch designs in hopes of improving integration [13]. Thus, an approach to cardiac patch engineering that improves cardiomyocyte alignment and anastomotic genetic cues could potentially improve cardiac patch survival and push the treatment towards further clinical relevance.

Innovation: Prevascularization of cardiac patches with grid patterned geometry has been shown to improve cardiac patch engraftment and anastomosis. Yet the grid pattern does not mimic native heart vasculature, and no study has yet examined the effects of various vessel geometries on patch anastomosis. Our approach is to develop cardiac patches with several different patterned geometries, and through experimentation, determine which pattern best promotes anastomosis and improved patch performance. Our experimental aims are designed to create and test the functionality of patches *in vitro* and *in vivo*, in order to establish if the vasculature geometry can maximize vasculogenesis gene expression, cardiomyocyte alignment, and ultimately anastomosis. While we hypothesize that the parallel patterned patches will anastomose most efficiently and produce the best cardiac patch engraftments, we believe that whatever the outcome of this research is it will inform future bioengineering techniques on the best way to construct a cardiac patch.

Research Design

Specific Aim 1: Prepatterning hiPSC-ECs using Laser Induced Forward Transfer (LIFT) to create cardiac patches with various vascular patterns in vitro and testing if printed patches match the expected outcomes.

Introduction: The ***objective*** of this aim is to develop and test the immediate integrity of various pre-patterned cardiac patches after printing. Our ***approach*** will be to develop these pre-patterned cardiac patches by using the LIFT bioprinting technique and human induced pluripotent stem cell derived-endothelial cells (hiPSC-ECs) and cardiomyocytes (hiPSC-CMs), to create the following well defined and controlled patterns: random, parallel, acute angle branches, grid, and zig zag. After culturing for 24 hours, immunostaining, confocal microscopy and a cell viability assay will allow us to observe if the cardiac patches remained viable and patterned . Our ***rationale*** for this aim is due to previous studies emphasizing the need for better pre-vascularized cardiac patch engraftment in vivo. The literature has already associated vascular geometry in cardiac patches with improved patch engraftment, that then helps to preserve cardiac function after myocardial infarction. The strategy laid out in this aim will develop pre-patterned and viable cardiac patches that we can then proceed with in Aim 2 to test patch functionality (Figure 1).

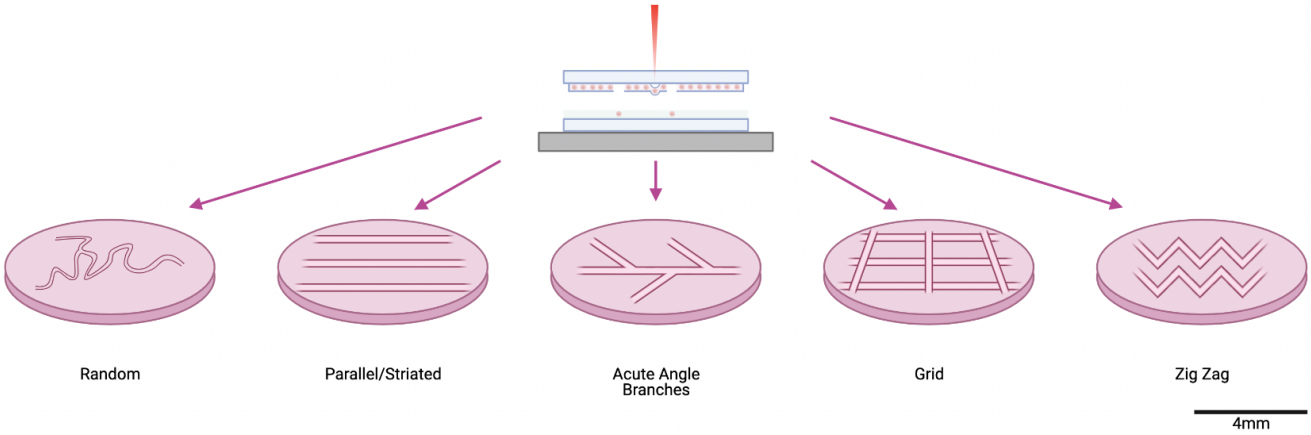

Figure 1. A graphical illustration of the desired experimental outcome for Aim 1.

Review of Relevant Literature: Cardiac patches are pieces of engineered functioning cardiac tissue that ideally is used to replace damaged myocardium and encourage recapitulated cardiac functioning and heart regeneration. The cardiac patches consist of two components: a substrate and therapeutic ingredients [14]. Therapeutic ingredients for cardiac patches can consist of cells (i.e. skeletal myoblasts, mesenchymal stem cells and human pluripotent stem cells) or bioactive molecules (i.e. growth factors, microRNA and extracellular vesicles) or a combination [14]. This proposal focuses on engineering cardiac patches with hiPSC-ECs and hiPSC-CMs. One of the main challenges however in engineering viable cardiac patches with cells is inducing proper prevascularization to support the nutritional needs of graft cells upon implantation, as well as inducing anastomosis between engineered and native vasculature. Several studies confirm that prevascularization and patterning of cardiac patches improve overall graft integration [15]. Our proposal seeks to pre-pattern patches to improve vascular anastomosis thereby improving patch engraftment, by using the laser-induced forward transfer (LIFT) 3D bioprinting technique, followed by a LIVE/DEAD cell viability assay, immunostaining, and confocal microscopy to ensure the expected outcome for the pre-patterned cardiac patches was achieved.

Rationale for this Approach: This aim is designed to focus on efficiently developing cardiac patches. This aim will provide differing vascular geometries that will be used to compare the effects vascular geometry has on cell functionality. We will carry out a cell viability assay, immunostaining and imaging

to analyze the patterns. Any experimentation before ensuring cell viability and the accuracy of the printed patterns would be futile, making this aim essential to complete prior to any in vitro testing.

Methodology:

Cell Differentiation Protocol

Human induced pluripotent stem cells, and human pluripotent stem cells differentiation kits for both cardiomyocytes and endothelial cells will be obtained from a commercial source. The cells will be differentiated according to the protocol recommended by the vendor before being incubated in the recommended mediums and placed in a humidified chamber with 5% CO_2 and at 37°C.

Preparing Cardiac Patch Substrate: Polyester urethane urea (PEUU)

The foundation for the patch will be polyester urethane urea that will be synthesized by the polymerization of polycaprolactone (PCL) and 1,4-diisocyanatobutane (BDI), with lysine ethyl ester or putrescine being used as chain extenders [16]. It will then be processed to have interconnected micropores by using thermally-induced phase separation (TIPS) techniques [16]. This specific technique promotes cell attachment and will allow us to control the pore size of the PEUU substrate, by changing the parameters (i.e. polymer solution concentration or quenching temperature) when preparing for separation, as needed [17]. The biodegradation rate of PEUU scaffolds depends on the porosity of the scaffolds [18]. Controlling the pore size will not only allow us to predetermine the amount of time before the PEUU scaffold is degraded, which would remove any immune responses associated with the presence of the scaffold in vivo after sufficient anastomosis, but we can also ensure the pore size obtained does not allow any seeded cells to enter the substrate. The PEUU substrate synthesized will mimic the elasticity and mechanical properties similar to native arteries. The PEUU material will be cut into circles with a radius of 4 mm, a thickness of 300 μm and an average pore size of 91 μm [19]. The cardiac patches will have both an inlet and outlet reservoir attached to the substrate [9, 19]. Both reservoirs will have channels branching from them where the hiPSC-ECs will be bioprinted, allowing for perfusion capabilities once lumen is fully formed and has anastomosed to the engineered channels at either end [9, 19].

LIFT Bioprinting of hiPSC-ECs onto Scaffold

Two aligned square glass slides (26 × 26 mm^2 and 1 mm thickness) will be used for every bioprinting process [19, 20]. The upper one, known as a donor slide, will be layered underneath with a laser-absorbing gold layer. The 4×10^6 hiPSC-ECs suspended in approximately 30 μl EGM-2, will be pipetted on top of the gold layer, and then with a blade coater, dispersed evenly across the gold surface of the donor slide [19, 20]. The collector slide aligned below will hold a PEUU scaffold that has been immersed in the BD Matrigel™ Matrix. A Nd:YAG-laser will be used during the bioprint process. The laser pulses will be focused prior to printing to produce an ablation spot size of 40 μm in diameter and then the patterns will be printed onto the PEUU scaffold [16]. Laser pulses will be focused through the donor slide onto the gold layer which will evaporate, causing an increase in gas pressure that will force the cells downward toward the collector slide. The space between the donor and collector slides will be set to 500 μm [19].

Cell Viability Assay

Directly after LIFT bioprinting, hiPSC-ECs on pre-patterned cardiac patches that do not have randomly seeded cardiomyocytes, will be rinsed with medium. A resazurin-based AlamarBlue™ reagent solution will be purchased commercially from Thermo Scientific (Cat: DAL1025). The AlamarBlue solution will be added to the medium, and the patch will be incubated at 37°C for four hours. In living metabolically active cells, resazurin is reduced to resorufin, which is red in color and fluorescent. Red fluorescence in the medium will be measured using a fluorescence-based plate reader. For each pattern, four cardiac patches will be tested for cell viability.

Immunostaining and Confocal Microscopy

Cardiac patches will be fixed with paraformaldehyde (PFA). The patches will be stained with polyclonal goat anti-Pecam 1 initially and then counterstained with antibodies for α-actinin. The patches will be rinsed thoroughly after staining with phosphate-buffered saline (PBS). The patches will then be placed on slides. They will then be ready to be analyzed using a commercially bought confocal microscope.

Experimental Design:

Activity 1: Lift 3D Bioprinting

We will pre-pattern the cardiac patches in random, parallel, acute angle branches, grid, and zig zag patterns by bioprinting onto a synthetic scaffold with the LIFT bioprinting technique. With other bioprinting techniques the clogging of the nozzle during printing is a major hindrance but, LIFT allows for high cell density during bioprinting while avoiding any nozzle clogging. [21, 22]. This technique also offers extremely high resolution and high cell viability post printing [21]. The LIFT technique has not been shown to pose a risk to the bioactivity of cells. Cell survival, cell proliferation, and cell DNA damage have been shown not to be significantly altered when cells were bioprinted using this technique [20]. LIFT 3D printing, even more importantly, enables the precise placement of cells by using a transfer substrate to absorb the UV light, causing partial vaporization of the support material and ultimately the deposition of the cells onto the desired substrate [23]. The cells that will be seeded on the patch will be hiPSC-ECs and hiPSC-CMs. iPSCs were chosen for their similarity to human embryonic stem cells but with the lack of ethical issues, as well as their patient specificity capabilities for future in vivo human implications [24]. The PEUU scaffold on the collector slide treated with a thin layer of matrigel, will provide an adhesion site for cells so they may stay positioned in the desired pattern [20]. The matrigel will also provide an adequate environment to prevent cell dehydration and cushion the impact during cell transfer. On completion of the cells being transferred from the first donor slide to the collector slide, the first donor slide will be replaced in order to print the second layer of hiPSC-ECs. For statistical purposes we will bioprint eight patches per pattern. The exact dimensions for how each pattern will be printed is as follows:

1. Randomly patterned geometry will be a product of co-seeding hiPSC-ECs and hiPSC-CMs without a set pattern on the cardiac patch away from the inlet and outlets. hiPSC-ECs alone will be pipetted near the inlet and outlet branches to encourage anastomosis between the cells and the engineered branches. These patches will be our control.
2. The parallel pattern may further increase host integration because this pattern better mimics the myocardium's native structure. hiPSC-ECs will be printed in two layers with 900 μm between parallel bioprinted lines.
3. The branched pattern could also serve to better mimic coronary structure in the body due to the already branched structure of native vasculature. hiPSC-ECs will be printed in two layers with one biprinted line down the center of the patch . Every 450 μm a hiPSC-ECs will be bioprinted at a 45° angle to the central bioprinted line. The lines will be printed alternating sides every 450 μm.
4. The grid pattern has been shown to improve cardiac patch engraftment after implantation by increasing host integration with the grid-oriented vasculature [9]. We will print hiPSC-ECs in two layers with 900 μm between grid lines.
5. The zigzag pattern will be an extra experimental design to further test how different geometries may affect overall integration. The hiPSC-ECs will be printed in two layers with 900 μm between sinusoidal lines.

hiPSC-CMs will be randomly seeded onto the scaffold after the bioprinting of hiPSC-ECs. 4.5×10^4 hiPSC-CMs will be pipetted onto a PEUU scaffold and allowed to adhere randomly. The patches will then be cultured in EGM-2 for either 24 hours then undergo a cell viability assay, or for 8 days to allow for vascularization to begin to take place.

Activity 2: Cell Viability Assay

While LIFT bioprinting is known to have high cell viability after printing, cell death still may occur depending on the chosen laser pulse energy, gap distance, focused laser spot size, thickness of the UV absorbing layer and the composition of the cell-containing layer [20, 21]. To determine if the cells are viable after patterning, the patches will be placed in EGM-2 for 24 hours after printing. Following this we will use the Alamar Blue viability assay and a fluorescence-based plate-reader to measure the percentage of living metabolically active cells.

Activity 3: Immunostaining and Confocal Imaging
Immunostaining can be used to identify unique cellular protein markers to help track specific cells. Immunostaining coupled with confocal microscopy will provide images of targeted cells with 3D optical resolution. We will stain the $CD31^{+}$ marker in the hiPSC-ECs and α-actinin (ACTN2) in the hiPSC-CMs. Confocal microscopy will then be done to observe the vascular formation and cardiomyocyte recruitment after LIFT bioprinting, to ensure that the patches maintained the pre-patterned geometry.

Expected Results: We expect that the cardiac patches will have viable cells with intact membranes after the bioprinting of the hiPSC-ECs. Cell viability for all patches is expected to be greater than 90%. After 8 days, we would expect to see that the hiPSC-ECs have recruited the surrounding randomly seeded hiPSC-CMs, during the process of vasculogenesis, to border the tubular structures being formed. The patches are also expected to maintain the desired pre-patterned vascular geometry.

Pitfalls:
Pitfall 1: It is possible that during vasculogensis the factors secreted and the signaling by the hiPSC-ECs may not only affect the immediately neighboring hiPSC-ECs and hiPSC-CMs, but it may also impact the hiPSC-ECs bioprinted adjacent or parallel to them. This may cause slight distortions in the desired pre-patterned vascular geometry.
Solution: If the hiPSC-ECs bioprinted adjacent or parallel to one another begin to anastomose toward each other and disrupt the patch geometry configuration, we could pattern the cardiomyocytes as well. Instead of randomly seeding cardiomyocytes, we could orient them by bioprinting them already bordering the endothelial cells instead of allowing them to be recruited. The presence of the cardiomyocytes would hopefully restrict the cross signaling and hiPSC-ECs secreted factors from reaching and have an effect on adjacent or parallel patterned hiPSC-ECs.

Pitfall 2: It is possible that the pore size of the PEUU substrate may be larger than the individually suspended cells when they are first bioprinted onto the scaffolds. This may allow for cells to enter the scaffolds, disrupting the patterned geometry we sought to create.
Solution: If the pore size of the PEUU substrate proves to obstruct the patterned geometry bioprinted onto the cardiac patches, the TIPS techniques' beginning parameters can be adjusted to shrink the pores of the scaffolds until they are appropriately sized.

Specific Aim 2: Testing patterned cardiac patches *in vitro* for perfusability, thrombogenicity, contractility, and differences in gene expression to ensure their usability for *in vivo* implantation as tissue matures.

Introduction: The ***objective*** of this aim is to analyze the functionality as well as quantitatively and qualitatively delineate the molecular and morphological differences between each of the patterned grafts *in vitro* in order to assess their potential for successful anastomosis in live rat models described in Aim 3. Our ***approach*** will be to assess established and measurable characteristics of cardiac patch proficiency such as perfusibility, angiogenic sprouting, non-thrombogenicity, contractility, cardiomyocyte alignment, and expression of genetic markers for endothelial and vascular development. Our ***rationale*** for this aim is due to the need for assessing the translatability of our grafts to *in vivo* models and the need to quantifiably differentiate the effects of different vascular patterns on the development and behavior of our patches, if possible. Characterizing our grafts in this

aim will give us a better understanding of any observable variations in graft anastomosis when implanted *in vivo*.

Review of Relevant Literature: Characterization of cardiac patches can entail assessment of numerous aspects, including the following:

(1) *Perfusion:* Perfusion a technique for maintaining adequate oxygen and nutrient availability during the manufacturing process. Perfusion in cardiac patches is also known to promote better de novo lumen formation (angiogenic sprouts), which has also been linked to better remodeling and anastomosis [9]. Reproducing the convective-diffusive properties of oxygen transport in native myocardial tissue has also been shown to improve CM survivability and contractile properties [25]. Furthermore, perfusing cardiac patches with rhythmic pulses as opposed to continuous static flow has been shown to enhance contractile properties [26]. Thus, we wish to ensure that all cardiac patches are perfusible before implantation in mice, and will consider perfusibility and angiogenic sprouting as indicators of anastomotic potential.

(2) *Thrombogenicity:* Non-thrombogenicity is a basic and well-documented functional necessity of any viable vascular network, particularly in cardiac patches, that is often checked before implantation of cardiac patches *in vivo*. Thrombogenicity of engineered vasculature is also a key inhibitor of adequate anastomosis [27].

(3) Contractility: Contractile function in response to electrical stimulation is an essential function of engineered cardiac patches and an important indicator of cardiomyocyte alignment in local tissue geometry [28]. We want to ensure that cardiomyocytes are able to contract properly before implantation and observe the effects of vascular patterning on cardiomyocyte alignment. Alignment of sarcomeres is also linked to better anastomosis in muscular tissue [13].

(4) *Genetic Expression:* Endothelial cells not only promote the vascularization and survival of cardiac patches, but they are also key mediators of signaling mechanisms that regulate cardiomyocyte activity [29, 30]. Variations in vascular patterning can have profound effects on the biological activity of organ grafts. Collagenous vascular patches engineered with various patterns implanted in infarcted rat hearts have been shown to cause unique vascular remodeling and unique gene expression profiles for genes associated with vascular and tissue development [9]. We will test for significant differences in gene expression in our vascularized cardiomyocyte grafts.

Methodology:

Perfusion of fluorescent beads: Vessels will be perfused with 50 µL of red fluorescent beads obtained from Thermo Fisher (F-13083) with a diameter of 1.0 µm each. Stored at a concentration of $1x10^{10}$ beads/µL, beads will be diluted in culture media at a 1:30 ratio for nutritional support of cells. Cardiac patches will be designed with both an inlet and outlet, similar to a microfluidic device. We will promote flow through our patches using a pulsatile perfusion bioreactor, similar to that described by Brown et al., to provide both mass transport and mechanical conditioning to the engineered tissue at physiologically relevant shear stresses and flow rates [26]. The main components of this bioreactor will consist of a reservoir of culture media, which will be attached to patch inlets for perfusion, a solenoid pinch valve, peristaltic pump, gas exchanger, and debubbling syringes. The perfusion loop will involve medium flowing from the reservoir into the patches through the inlet. The pinch valve will be attached to the outlet such that pulsatile flow can be controlled. The pump, which will be attached to the perfusion loop after the valve, will run for 0.5s intervals while the valve is closed. This will result in pressure to build up in the perfusion chamber and patch contraction, forcing all fluid out of the patch and through the gas exchanger before returning to the reservoir. Opening of the valve, at a frequency of 1Hz, will cause the patches to relax, allowing for medium to flow back into the patch from the reservoir. A debubbling syringe with excess culture medium will be attached to the perfusion loop before and after the cardiac patch in order to ensure that there are no bubbles in the flow-through. Fluorescent beads will be added to the medium reservoir at the relevant time points for imaging. Pump settings will be set to induce a flow rate of 500µm/s to mimic native myocardium—a flow rate

which will also help us achieve the recommended wall shear stress of 10-30 dyne/cm^2 at this size scale [9] . A Nikon high resolution wide field microscope will be used to capture fluorescent time series imaging of the beads and bead velocity will be calculated from this imaging via manual particle tracking using ImageJ software. Likewise, ImageJ software will be used to measure perfusion area for each of the patches from time series imaging.

Whole-blood perfusion for non-thrombogenic analysis: Fresh citrate-stabilized, ABO-matched blood will be obtained from the Massachusetts General Hospital Blood Donor Center. Platelet rich plasma (PRP) will be isolated and platelets in the PRP will be labeled with fluorescein isothiocyanate-conjugated CD41a antibody obtained from BD Pharmingen. The labeled PRP will then be reconstituted with red blood cells and buffy coat for perfusion in vasculature. Perfusion will take place for 30 minutes such that wall shear stress is at the recommended 10-30 dyne/cm^2 [9] . Nikon high resolution wide field microscope will be used to capture fluorescent time series imaging of the platelets and assess any platelet accumulation on vessel walls. After blood perfusion, patches will be washed with PBS for removal of excess blood suspension and then fixed in formaldehyde. Fixed patches will then be stained for CD31 and von Willebrand factor and imaged via confocal microscopy to ensure endothelial survival. Platelet adhesion will also be quantified in image stacks by measuring CD41a+ fluorescent signal and normalizing fluorescent area to surface area of vessel wall.

Thrombogenic Activation: For stimulation of thrombogenesis, 50ng/ml phorbol myristate acetate (PMA) will be perfused through vessel lumen for 30min prior to washing with PBS and perfusing whole blood as described earlier.

Force Generation: At days 7 and 14, patches will be pinned to a fixed tissue holder at one end and to a PDMS floating holder connected to the optical force transducer at the other end. Two electrodes connected to a cardiac stimulator will be placed on either side and a 10-ms stimulus will be applied at an amplitude of 3V to induce contraction at a rate of 60 beats per minute. Single twitch parameters such as amplitude, the time-to-peak twitch (TPT, from onset of electrical stimulus to time of peak twitch), and half relaxation time (from time of peak twitch to 50% recovery time) will be collected or derived from force traces.

Sarcomere Imaging
Patches will be stained with primary antibodies for sarcomeric anti-α-actinin and secondary antibody tetramethylrhodamine-conjugated goat anti-mouse IgG obtained from Sigma-Aldrich. We will look for positive labeling of Z-discs for sarcomeric α-actinin and the presence of striations in the immunofluorescence images captured using a confocal microscope.

RNA Isolation and RNAseq Analysis:
We will first dissociate the cells in our patches using a MACS® Tissue Dissociation Kit and then isolate the endothelial cells using immunomagnetic cell separation with positive selection for *Pecam1* (CD31), the most common antibody marker for endothelial cells. We will ensure 90% viability of cells and then conduct single cell prep for sequencing using the 10x Chromium Controller according to the manufacturer's specifications. RNA extraction will be done using RNAeasy mini kit and protocol obtained from Qiagen. We will then assess RNA concentration and quality using Nanodrop spectrophotometer readings and RNA with adequate purity will be sequenced using Illumina TruSeq. From this data we will compare the patch sequences using the DESeq2 package in R to find significant differences in gene expression profiles and then we will curate this analysis of different genes with the Gene Set Enrichment Analysis Molecular Signatures Database (v7.4) to analyze particular pathway upregulation and downregulation.

Experimental Design:
Activity 1: Perfusibility and Angiogenic Sprouting

In order to determine the patency of our vessels over time, we will examine the perfusibility and flow dynamics of our engineered vascular constructs by perfusing red fluorescent beads through vessel inlets via a pulsating bioreactor. We will measure perfusion velocity, perfusion area, angiogenic sprouts and structural remodeling at 4,7, and 14 days for 5 patches of each pattern. Bead velocity will be measured both in patterned vessels and their respective angiogenic sprouts using manual particle tracking and fluorescent time series imaging. Using the self-assembled vasculature as a control, we will examine if certain vascular patterns have higher perfusion velocity which is inversely related to the vascular resistance--a common metric for evaluating vascular patency. It has been shown that perfusion promotes better angiogenic sprouting which, in turn, leads to better vascular remodeling and anastomosis. The degree of angiogenic sprouting has also been used as a proxy for anastomotic potential [9]. Thus, over the course of perfusion we will manually count angiogenic sprouts as well as measure their length and diameter over the course of patch maturation at 4-, 7-, and 14-day time points using confocal z-stack imaging for 5 patches of each pattern. Angiogenic sprouts will be quantified since the extent of angiogenic sprouting is an indicator of anastomotic potential. Although they may not allow complete flow-through, beads can still be imaged in angiogenic sprouts to confirm lumen formation and previous literature has shown that increased angiogenic sprouting (regardless of complete loop formation) reduces average flow velocity throughout the entire patch due to the increase in surface area [9]. It is expected that total perfusion area will increase over time in some constructs due to sprouting and vascular remodeling, which will decrease vascular resistance and allow for more efficient perfusion. We will measure the total area of perfused beads using imageJ software. Constructs with significantly higher degrees of angiogenic sprouting and higher perfusible area than self-assembled vasculature will be expected to induce quicker anastomosis in mouse model implants.

Activity 2: Non-thrombogenicity

To further examine the patency of the engineered vasculature over time we will examine the non-thrombogenicity of the patterned vessels to gauge their usability *in vivo.* We will do this by analyzing interactions between the hiPSC-EC derived vessels and citrate-stabilized, ABO-matched whole blood with platelets labeled with fluorescein isothiocyanate-conjugated antibodies to CD41a. Blood will be perfused through the inlets for 30 mins at 4,7, and 14 day time points. We will examine the blood perfusion for large aggregates of platelets using a Nikon high-resolution wide-field microscope to visualize red blood cell movement and platelet accumulation near the vessel walls. Platelet adhesion will be quantified by measuring the area of fluorescent signal from CD41a+ normalized to the vessel wall surface area; small amounts of adherence to vessel walls will be acceptable. After testing for non-thrombogenicity, we test to see if engineered vasculature can be converted to a thrombogenic state in response to physiological stimuli. Thrombogenicity of vasculature is an important part of the immune response and is used by the body as a mechanism for minimizing blood loss, improving wound healing, etc. Thus, it is important not only to engineer perfusable vasculature, but also vasculature that can respond to physiological stimuli and induce an immune response. Therefore, testing for thrombogenic activation is an essential aspect of functional vasculature. We will activate the hiPSC-ECs with phorbol myristate acetate (PMA) and test for platelet adhesion after 30 minutes of blood perfusion. After blood perfusion, we will wash vessels to remove excess blood suspension, fix the patches in formaldehyde, and immunohistochemically stain them for CD31 and VWF to visualize and measure protein expression of endothelial markers. We expect to demonstrate that vessels are non-thrombogenic and can convert to thrombogenicity as response to physiological stimuli while maintaining endothelial markers. Any constructs that do not meet this standard will not be implanted in animal models.

Activity 3: Contractility

To further evaluate the function of the engineered constructs we will measure the contractile force and assess the sarcomere alignment of the cardiac patches. Patches will be measured for a twitch force when paced with field stimulation mimicking that of the heart. While twitch force per input CMs has been used as a measure of patch efficiency and a measure of proper cardiomyocyte alignment, we

will simply look at twitch force given that equal amounts of CMs have been input into our patches [31]. After comparing patch contractile forces to each other and to the randomly vascularized control patch, we will also compare patch contractility to native cardiac tissue in the rat hearts. It is expected that patches with better cardiomyocyte alignment and remodeling in relation to the engineered vasculature will likely display higher twitch force per unit CM over time. While contractile force will be used as a proxy for cardiomyocyte alignment, *a*ctual alignment will be visualized and quantified with confocal immunofluorescent imaging of cardiomyocyte fibers and sarcomere structures using troponin and myosin heavy-chain-7 stains. These stains should also help us to visualize the intercalated discs between cardiomyocytes. We will quantify cardiomyocyte alignment from cardiomyocyte imaging by measuring the angle of deviation from a normalized axis using standard imaging software.

Activity 4: Gene Expression

First, we will dissociate our patches and isolate endothelial cells. We will then extract RNA samples for analysis. To confirm the quality of RNA samples prior to RNASeq analysis we will perform qPCR analysis to look for differential expressions of VEGFA, ANGPTL4, and ENO2 which have been shown to be significantly different in anastomotic cultures *in vitro* [9]. Samples with significantly different expression of these genes will be further characterized by RNAseq and differential expression analysis. RNA samples will be collected from patches after 14 days of *in vitro* culture (n=6 for each pattern that passes the pilot analysis). Pro-anastomotic genes including enzymes ENO2, ALDOA, and ARG2; growth factors VEGFA and VEGFB; angiocrine factors ANGPTL4 and IGFBP5; and peptidases such as MME and MMP9 have all been shown to differentiate anastomotic cultures of blood vessels from non-anastomotic culture [9]. In addition, *in vitro* anastomotic cultures have been shown to express significant upregulation in glycolysis, hypoxia, tumor necrosis factor-α signaling via nuclear factor-κB, mammalian target of rapamycin C1 (mTORC1) signaling, and epithelial–mesenchymal transition (EMT) [9]. For this reason we plan to perform differential expression analysis and gene ontology terminology analysis to assess differences in gene signatures between patterned grafts and the spontaneously assembled vasculature as well as differences between the variously patterned grafts themselves. Finally, anastomotic constructs have been shown to have significant upregulation of mTOR signaling, EIF2 signaling, IL-8 signaling, hypoxia-inducible factor-1α signaling, VEGF signaling, EMT regulation, glycolysis, endothelin-1, Wnt/β-catenin, Neuregulin, and C-X-C chemokine receptor 4, and significant downregulation of phosphatase and tensin homolog, Notch, and apoptosis signaling. Therefore, we will perform canonical pathway analysis to identify differences in endothelial phenotypes and vascular development between our patches.

Expected Results: Vascular remodeling and angiogenic sprouting will likely decrease vascular resistance allowing for efficient perfusion. We expect that perfusion dynamics will change between patches based on vascular geometry with parallel patterned vessels having the most efficient perfusion. In turn, we expect angiogenic sprouting to be higher within patches that have more efficient perfusion. This increased sprouting will, further, result in more efficient perfusion. We expect that all patches will have similar non-thrombogenic activity and thrombogenic activation potential. Thus, we expect to implant all patches into murine models. However, we expect to be able to differentiate between patches based on contractility and genetic expression of relevant phenotypes and pathways. We expect the parallel patterned patch to have better cardiomyocyte and sarcomere alignment leading to stronger twitch force measurement. Likewise, we expect the parallel patterned patch to show the most significant upregulation of pro-anastomotic genes and downregulation of Notch and apoptosis signaling. All patches that are perfusible, non-thrombogenic will contractility over will be implanted in Aim 3.

Pitfalls:

Pitfall 1: There is a chance that we cannot achieve sufficient perfusability in the randomly patterned patch. Due to the random nature of vessel formation, the endothelial cells may not end up connecting with the engineered inlets and outlets.

Solution: Although this seems unlikely given that perfusible, random vasculature was achieved using this method in a previous study, if we are unable to get adequate perfusion then we can introduce slightly more control over the randomly patterned vasculature such as inducing directionality of vessel formation using an electric field to try to force vessels to connect at inlets and outlets [9].

Pitfall 2: We may not find significant differences in contractility and cardiomyocyte alignment between different patterns of patches. If the blood vessels do not seem to affect cardiomyocyte alignment then we will have to manually engineer cardiomyocyte alignment to ensure contractility of patches.
Solution: We can also do imaging of calcium transients to further characterize the patches if original results can not differentiate between them. If this fails, we will pattern the cardiomyocytes to further isolate effects of vascular patterning on gene expression and anastomosis *in vivo.*

Pitfall 3: We may not find significant differences in gene expression between the patterned patches *in vitro* due to the fact that they are not undergoing any anastamosis in culture.
Solution: We will still proceed with *in vivo* testing for all patches that are non-thrombogenic and perfusible given that gene expression may change in relation to host vasculature.

Specific Aim 3: Performing an *in vivo* study in a rat model of myocardial infarction to investigate and compare the efficacy of various cardiac patch patterns.

Introduction: The *objective* of this aim is to analyze and compare the efficacy, measured through anastomosis and perfusion, in a rat model. Our *approach* will be to perform various murine *in vivo* assays to assess and compare the efficacy of each successful patch from Aim 2. Our *rationale* for this aim is that animal models provide more biologically relevant data and that this initial small animal model may pave the way forward towards larger animal models, advancing towards translational applications. The experiments that will be carried out for this aim will identify the optimal endothelial cell design for cardiac patches *in vivo* (Figure 2).

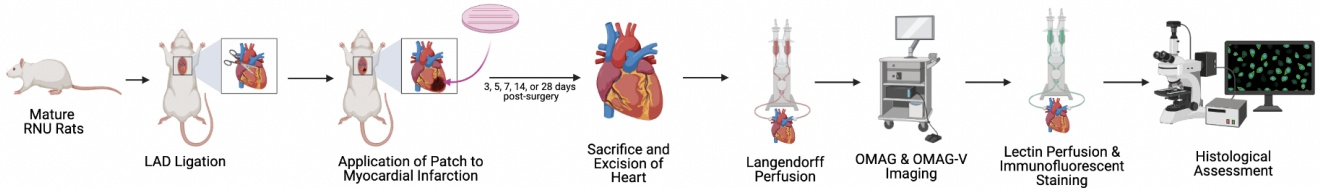

Figure 2. Experimental Design for Aim 3.

Review of Relevant Literature: The evaluation of cardiac patches in murine models has been successfully performed in various papers. In order to investigate the efficacy of a patch *in vivo*, standard practice dictates the induction of a MI and the immediate application of the cardiac patch. Standard *ex vivo* analysis techniques include histological analysis using lectin perfusion and immunofluorescent staining. Additionally, Optical Coherence Tomography(OCT)-Based Optical Microangiography (OMAG), while not as ubiquitously used in the field, can convey important information regarding flow and perfusion in the cardiac patch and new coronary vasculature, which is often overlooked in standard histological analysis [9].

Rationale for this Approach: This aim focuses on comparing various cardiac patch designs *in vivo* in order to assess their efficacy and provide potential translationally relevant conclusions regarding endothelial cell pattern design.

Methodology:
Rowett Nude (RNU) Rat
We will perform all *in vivo* testing using the Rowett Nude (RNU) Rat, obtained from Charles River Laboratories (Strain Code: 316). This rat is commonly used for xenograft experiments, as it is T-cell

deficient. Rats will be purchased at 15 weeks of age and undergo surgery at 24 weeks of age, as they reach maturity at approximately 1 year [32].

Left Anterior Descending Coronary Artery Ligation
Rats will be anesthetized and undergo thoracotomy. We will then induce MI by permanently ligating the left anterior descending (LAD) coronary artery. This is a commonly used technique for modelling MI *in vivo* [33].

Cardiac Patch Implantation
We will implant the cardiac patch immediately after LAD ligation by suturing it onto the epicardium of the left ventricle using 8-0 Sterile Micro Suture, purchased from AROSuture™. Following suturing, excess blood will be dabbed away and the chest will be stitched closed.

Quantification of Vascular Structure and Fluid Velocity
Following excision, we will immediately perfuse with 10% i.v fat emulsion (Intralipid 10%), purchased from RxList Inc. Perfusion pressure will be kept at 90 mmHg for the duration of OMAG assessment. Images will be viewed and captured in a square, 2.25 mm^2, field of view and with the conventional OCT apparatus [34]. Both OMAG and OMAG-based capillary velocimetry (OMAG-V) will be used to obtain images of vascular structure and the velocity of fluid within the patches. For OMAG, we will obtain a 3D dataset by utilizing raster beam scanning for 15 seconds at a frame rate of 280 frames per second. We will quantify vessel density by determining volumetric vasculature maximum intensity projections (MIPs) as a percentage of the 3D image [9]. For OMAG-V, we will utilize an adaptive regression filter, which identifies signals from moving Intralipid 10% particles, while ignoring signals from static tissue. The frequency of these particles will be estimated by calculating the correlation between eigenvectors from sequential frames produced by the regression filter. The velocity of the flow within the vessels will be calculated through its established linear relationship with the frequency of particle movement through the vessel [35]. Perfusion rates will be quantified by multiplying the obtained velocity readings by the perfused area in which those readings were measured. Then, these rates will be normalized based on the perfusion of a healthy region of the same rat's heart.

Histological Analysis
We will flush out the heart with phosphate-buffered saline (PBS) for 10 minutes in order to clear out any remaining Intralipid 10% from OMAG analysis. We will then perfuse with with a 1:1 mixture of 8 µg/mL Fluorescein Griffonia simplicifolia Lectin I (GSL I) and 8 µg/mL Rhodamine Ulex europaeus Agglutinin I (UEA I), purchased from Vector Labs. The hearts will be flushed out with PBS for 10 minutes once again.

We will slice 4 µm sections from the excised hearts and stain for picrosirius red (stains collagenous regions, such as infarct) with a counterstain of fast green (stains healthy tissue) [9]. We will view these samples using a NanoZoomer digital slide scanner, obtained from Hamamatsu. We will quantify infarct size by normalizing infarct regions to left ventricle size. We will characterize inflammatory response by measuring macrophage (CD68+) infiltration into the cardiac patch. We will use CD68 antibodies to stain for macrophages, hematoxylin as a counterstain to identify all nuclei, and a compound microscope to image results. Infiltration will be quantified by calculating the percent of cells that are macrophages [9].

We will also slice 2 mm sections from the excised hearts. These samples will be blocked and permeabilized using natural donkey serum and 0.5% Triton X-100, purchased from Thermo Fisher Scientific. We will incubate them overnight with primary antibodies (mouse mAb to rhodamine, goat Ab to GSL I, rabbit pAb to hCD31). We will then use appropriate Alexa Fluor® conjugated secondary antibodies for immunofluorescent-based stains. We will image all results using x20 confocal microscopic imaging, except for quantification of patch size, which will be viewed under brightfield imaging [9].

Cell Viability
We will perform a terminal deoxinucleotidyl transferase-mediated dUTP-fluorescein nick end labeling (TUNEL) assay and co-stain with α-actinin in order to label human cardiomyocytes and identify apoptotic cells within the cardiac patch region [9]. We will also stain with Hoechst in order to label all nuclei [9].

Experimental Design:
Activity 1: Cardiac Patch Implantation
Immediately after LAD-ligation, rats will receive one of the successful patch designs from Aim 2. n = 20 RNU rats for each patch design. After 3, 5, 7, 14, or 28 days (n = 4 for each group for each time point), we will remove the heart and patch for analysis. We decided to include the first three time points because previous studies that investigated anastomosis have lasted 3-7 days post surgery [8,9]. We are also interested in investigating the last time point of 14 days to determine if any additional substantial remodeling occurs longterm. Our control group will be the cardiac patch with randomly seeded endothelial cells. Quantification of results will be discussed in the following activities.

Activity 2: OMAG Analysis
We will sacrifice the rats (day 3, 5, 7, 14, or 28; n = 4 for each group at each time point), exercise the hearts, and perfuse *ex vivo* in order to perform OMAG and OMAG-V assessment. While standard approaches—dependent on red blood cell presence or lectin staining—provide meaningful information about anastomosis, they do not provide direct information regarding flow and perfusion in the patch and new coronary vasculature. We will quantify vessel density by calculating volumetric vasculature MIPs as a percentage of the obtained images. We will quantify fluid velocity within the vessels by using a regression filter to identify the signals of moving particles and normalizing to healthy regions of the heart. We expect to see increased vessel density and fluid flow velocity in the cardiac patches with endothelial cells that were patterned in a parallel manner, as compared to random seeding and other designs. We further expect to see increased density and velocity at earlier time points for the parallel designs, as compared to the random one and other designs.

Activity 3: Infarct Characterization
We will characterize the infarct for size and inflammatory response within the cardiac patch region for all excised hearts (n = 4 for each group at a given time point). We will image two sections for each heart. We expect to see no significant differences between groups for infarct size and inflammatory response within the patch. This will ensure that these factors are not confounding the anastomosis and perfusion data.

Activity 4: Immunofluorescent-Staining and Histological Assessment
We will perfuse *ex vivo* hearts with GSL I and rhodamine UAE I, which bind to rat endothelial cells and human endothelial cells, respectively. We will then obtain slices of each heart and wash and block the samples. The following primary antibodies will then be used in order to further quantification of patch integration:

- Mouse mAb to rhodamine: will bind to and allow for detection of perfused human vessels within the cardiac patch.
- Goat Ab to GSL I: will allow for detection of perfused endothelial cells from either the patch or the host (while GSL I is specific to rat endothelial cells, current anti-GSL I antibodies are not lectin-specific).
- Rabbit pAb to hCD31: will bind to all human endothelial cells, regardless of whether or not they are perfused.

We will quantify the density and size of human cell vasculature within the patch by imaging slides that were stained for human hCD31. We will analyze two sections from each heart and we expect to see

no significant change in endothelial tissue density and lumen size within the patch across patch designs. We will quantify the density and size of *perfused* vasculature on infarcted and on healthy regions of the heart by imaging slides that were stained for GSL I or rhodamine UEA I. We will analyze two infarct sections. We expect to see greater density and size of perfused vessels in the cardiac patch that was designed with parallel endothelium, as compared to the other pre-patterned designs and the random seeding control patch. We also expect density and size to increase over time in all groups, though we anticipate that the parallel design will achieve increased density and size at an earlier time than the other designs.

We will quantify cardiomyocyte viability by identifying the percentage of all cells in the patch that are apoptotic (TUNEL+). We will quantify this percentage by counting TUNEL+ cells and dividing by the total number of cardiomyocytes, which will be quantified by counting the nuclei stained by Hoechst. We expect apoptosis to increase with time from day 3 to day 7, though we anticipate that apoptosis will be less in the patch with parallel vasculature design, as compared to the other patch designs. We expect that apoptosis will remain relatively unchanged between day 14 and 28.

Expected Results:
The experiments described above are expected to provide insight regarding the speed and extent of anastomosis across various patch designs. We expect that the parallel endothelial pattern will show increased perfusable vascular density from the OMAG experiment and the histological staining, increased fluid velocity within vessels from the OMAG-V experiment, and increased cell viability from the TUNEL+ assay, indicating an increase in the speed and extent of anastomosis. We also hope that the results from the later time points (day 14 and day 28) will provide insight to how cardiac patch remodelling occurs over time *in vivo*. From the histological staining, we expect that overall vascular density, including perfusable and non-perfusable vasculature, will be similar across groups. We also expect to see no significant differences in infarct size and inflammatory response.

Pitfalls:
Pitfall 1: It is possible that the parallel patch design is not successful in Aim 2, thereby rendering our hypothesis that parallel vasculature design will result in increased and earlier anastomosis impossible to test in Aim 3.
Solution: If only the parallel patch design is unsuccessful in Aim 2, we may revise our hypothesis to claim that a certain, yet to be determined, pre-patterning design for cardiac patches will result in increased and earlier anastomosis and that the experiments performed in Aim 3 will uncover this design. If multiple designs are unsuccessful in Aim 2, we will repeat Aims 1 and 2 until cardiac patches that are suitable for implantation are developed.

Pitfall 2: It is possible that there is low cell survivability for all patches and few cells survive *in vivo* and, thus, cannot perfuse and anastomosis.
Solution: If few cells survive in many or all of the patch designs, we could reconsider patch redesign with growth factors and/or patterned CMs.

References

[1] World Health Organization. (2020, December 9). The top 10 causes of death. https://www.who.int/news-room/fact-sheets/detail/the-top-10-causes-of-death.

[2] A Maziar Zafari, M. D. (2020, December 5). Myocardial Infarction. Practice Essentials, Background, Definitions. https://emedicine.medscape.com/article/155919-overview#:~:text=Approximately%201.5%20million%20cases%20of%20myocardial%20infarction%20(MI)%20occur%20annually.(STEMI)%20has%20progressively%20increased.

[3] Price, E. L., Vieira, J. M., & Riley, P. R. (2019). Model organisms at the heart of regeneration. Disease Models & Mechanisms, 12(10), dmm040691. https://doi.org/10.1242/dmm.040691

[4] Levenberg, S., Rouwkema, J., Macdonald, M. et al. Engineering vascularized skeletal muscle tissue. Nat Biotechnol 23, 879–884 (2005). https://doi.org/10.1038/nbt1109

[5] Stevens, K. R., Kreutziger, K. L., Dupras, S. K., Korte, F. S., Regnier, M., Muskheli, V., … Murry, C. E. (2009). Physiological function and transplantation of scaffold-free and vascularized human cardiac muscle tissue. Proceedings of the National Academy of Sciences, 106(39), 16568–16573. https://doi.org/10.1073/pnas.0908381106

[6] Tulloch, N. L., Muskheli, V., Razumova, M. V., Korte, F. S., Regnier, M., Hauch, K. D., … Murry, C. E. (2011). Growth of Engineered Human Myocardium With Mechanical Loading and Vascular Coculture. Circulation Research, 109(1), 47–59. https://doi.org/10.1161/circresaha.110.237206

[7] Sekine, H., Shimizu, T., Hobo, K., Sekiya, S., Yang, J., Yamato, M., … Okano, T. (2008). Endothelial Cell Coculture Within Tissue-Engineered Cardiomyocyte Sheets Enhances Neovascularization and Improves Cardiac Function of Ischemic Hearts. Circulation, 118(14_suppl_1). https://doi.org/10.1161/circulationaha.107.757286

[8] Wang, L., Serpooshan, V., & Zhang, J. (2021). Engineering Human Cardiac Muscle Patch Constructs for Prevention of Post-infarction LV Remodeling. Frontiers in Cardiovascular Medicine, 8. https://doi.org/10.3389/fcvm.2021.621781

[9] Redd, M. A., Zeinstra, N., Qin, W., Wei, W., Martinson, A., Wang, Y., … Zheng, Y. (2019). Patterned human microvascular grafts enable rapid vascularization and increase perfusion in infarcted rat hearts. Nature Communications, 10(1). https://doi.org/10.1038/s41467-019-08388-7

[10] Nguyen, A.H., Marsh, P., Schmiess-Heine, L. et al. Cardiac tissue engineering: state-of-the-art methods and outlook. J Biol Eng 13, 57 (2019). https://doi.org/10.1186/s13036-019-0185-0

[11] Engelmayr GC, Jr, et al. (2008) Accordion-like honeycombs for tissue engineering of cardiac anisotropy. Nat Mater 7(12):1003–1010.

[12] Vollert, I., Seiffert, M., Bachmair, J., Sander, M., Eder, A., Conradi, L., ... & Eschenhagen, T. (2014). In vitro perfusion of engineered heart tissue through endothelialized channels. Tissue engineering Part A, 20(3-4), 854-863.

[13] Juhas, M., Engelmayr, G. C., Fontanella, A. N., Palmer, G. M., & Bursac, N. (2014). Biomimetic engineered muscle with capacity for vascular integration and functional maturation in vivo. Proceedings of the National Academy of Sciences, 111(15), 5508-5513.

[14] Mei, X., & Cheng, K. (2020). Recent Development in Therapeutic Cardiac Patches. Frontiers in Cardiovascular Medicine, 7. https://doi.org/10.3389/fcvm.2020.610364

[15] Montgomery, M., Zhang, B., & Radisic, M. (2014). Cardiac Tissue Vascularization. Journal of Cardiovascular Pharmacology and Therapeutics, 19(4), 382–393. https://doi.org/10.1177/1074248414528576

[16] Guan, J., Fujimoto, K. L., Sacks, M. S., & Wagner, W. R. (2005). Preparation and characterization of highly porous, biodegradable polyurethane scaffolds for soft tissue

applications. Biomaterials, 26(18), 3961–3971. https://doi.org/10.1016/j.biomaterials.2004.10.018

[17] Liu, S. Q., & Kodama, M. (1992). Porous polyurethane vascular prostheses with variable compliances. *Journal of Biomedical Materials Research*, *26*(11), 1489–1502. https://doi.org/10.1002/jbm.820261108

[18] Guan, J., Sacks, M. S., & Wagner, W. R. (n.d.). Development of a highly porous, flexible and biodegradable poly(ester urethane)urea scaffold for tissue engineering. *Proceedings of the Second Joint 24th Annual Conference and the Annual Fall Meeting of the Biomedical Engineering Society [Engineering in Medicine and Biology]*. https://doi.org/10.1109/iembs.2002.1137058

[19] Gaebel, R., Ma, N., Liu, J., Guan, J., Koch, L., Klopsch, C., … Steinhoff, G. (2011). Patterning human stem cells and endothelial cells with laser printing for cardiac regeneration. Biomaterials, 32(35), 9218–9230. https://doi.org/10.1016/j.biomaterials.2011.08.071

[20] Koch, L., Kuhn, S., Sorg, H., Gruene, M., Schlie, S., Gaebel, R., … Chichkov, B. (2010). Laser Printing of Skin Cells and Human Stem Cells. Tissue Engineering Part C: Methods, 16(5), 847–854. https://doi.org/10.1089/ten.tec.2009.0397

[21] Puluca, N., Lee, S., Doppler, S., Münsterer, A., Dreßen, M., Krane, M., & Wu, S. M. (2019). Bioprinting Approaches to Engineering Vascularized 3D Cardiac Tissues. Current Cardiology Reports, 21(9). https://doi.org/10.1007/s11886-019-1179-8

[22] Calvert P. MATERIALS SCIENCE: printing cells. Science. 2007;318(5848):208–9.

[23] Tran, V., & Wen, X. (2014). Rapid prototyping technologies for tissue regeneration. Rapid Prototyping of Biomaterials, 97–155. https://doi.org/10.1533/9780857097217.97

[24] M. Pad, L. Nanni, A. Lahti, S. Severi, K. Aalto-Setala and J. Hyttinen, "Computer vision for human stem cell derived cardiomyocyte classification: The induced pluripotent vs embryonic stem cell case study," 2011 Computing in Cardiology, 2011, pp. 569-572.

[25] Radisic M, Yang L, Boublik J, Cohen RJ, Langer R, Freed LE, et al. Medium perfusion enables engineering of compact and contractile cardiac tissue. Am J Physiol Heart Circ Physiol. (2004) 286:H507–16. doi: 10.1152/ajpheart.00171.2003

[26] Brown MA, Iyer RK, Radisic M. Pulsatile perfusion bioreactor for cardiac tissue engineering. Biotechnol Prog. (2008) 24:907–20. doi: 10.1002/btpr.11

[27] Raimund H.M. Preidl, Silvy Reuss, Friedrich W. Neukam, Marco Kesting, Falk Wehrhan, Endothelial inflammatory and thrombogenic expression changes in microvascular anastomoses – An immunohistochemical analysis, Journal of Cranio-Maxillofacial Surgery, 2021, ISSN 1010-5182, https://doi.org/10.1016/j.jcms.2021.02.006.

[28] Bian W, Juhas M, Pfeiler TW, Bursac N. Local tissue geometry determines contractile force generation of engineered muscle networks. Tissue Eng Part A. 2012 May;18(9-10):957-67. doi: 10.1089/ten.TEA.2011.0313. Epub 2012 Jan 4. PMID: 22115339; PMCID: PMC3338113.

[29] Talman V, Kivelä R. Cardiomyocyte-endothelial cell interactions in cardiac remodeling and regeneration. Front Cardiovasc Med. (2018) 5:101. doi: 10.3389/fcvm.2018.00101

[30] Zakharova IS, Zhiven MK, Saaya SB, Shevchenko AI, Smirnova AM, Strunov A, et al. Endothelial and smooth muscle cells derived from human cardiac explants demonstrate angiogenic potential and suitable for design of cell-containing vascular grafts. J Transl Med. (2017) 15:54. doi: 10.1186/s12967-017-1156-1

[31] Zhang J, Wilson GF, Soerens AG, et al. Functional cardiomyocytes derived from human induced pluripotent stem cells. Circulation Research. 2009;104(4):e30–41.

[32] Sengupta P. (2013). The Laboratory Rat: Relating Its Age With Human's. International journal of preventive medicine, 4(6), 624–630.

[33] Reichert, K., Colantuono, B., McCormack, I., Rodrigues, F., Pavlov, V., & Abid, M. R. (2017). Murine Left Anterior Descending (LAD) Coronary Artery Ligation: An Improved and Simplified Model for Myocardial Infarction. Journal of visualized experiments : JoVE, (122), 55353. https://doi.org/10.3791/55353

[34] Choi, W. J., Wang, H., Wang, R. K. (2014). Optical coherence tomography microangiography for monitoring the response of vascular perfusion to external pressure on

human skin tissue. Journal of Biomedical Optics, 19(05), 1. https://doi.org/10.1117/1.jbo.19.5.056003

[35] Wang, R. K., Zhang, Q., Li, Y., & Song, S. (2017). Optical coherence tomography angiography-based capillary velocimetry. Journal of Biomedical Optics, 22(6), 066008. https://doi.org/10.1117/1.jbo.22.6.066008